

# How to Identify Pre-Protostellar Cores

Erik M. Gregersen<sup>1</sup>

Department of Physics and Astronomy, McMaster University, Hamilton, ON L8S 4M1, Canada

Neal J. Evans II<sup>2</sup>

Department of Astronomy, The University of Texas at Austin, Austin, TX 78712-1083

L<sup>A</sup>T<sub>E</sub>Xed at 1177 min., December 23, 2021

## ABSTRACT

We have observed the  $\text{HCO}^+$   $J = 3 - 2$  line toward 17 starless cores selected from the list of Ward-Thompson et al. (1994). Six of these cores have line asymmetries indicative of collapse. The excess of blue-skewed profiles over red-skewed profiles is at least as large as that found in samples of Class 0 and early Class I sources. The observed line profiles have the same narrow linewidths and small peak temperatures predicted for young sources in evolutionary models, but the blue/red ratios, like those of older sources, are higher than models predict. The infall signature also occurs over large scales, suggesting that these cores have overall inward motions. We have divided these starless cores into two groups based on the continuum photometry of Ward-Thompson et al. and our  $\text{HCO}^+$  data. We find stronger  $\text{HCO}^+$  emission among the cores detected in the submillimeter and all the blue-skewed line profiles are in this group, supporting the suggestion of Ward-Thompson et al. that these are the pre-protostellar cores.

*Subject headings:* Star formation

## 1. INTRODUCTION

For years, the protostellar collapse stage had been an impenetrable mystery, until Walker et al. (1986) observed line profiles indicative of collapse in IRAS 16293-2422. Menten et al. (1987) disputed this interpretation and claimed that the asymmetric line profiles of Walker et al. were caused by rotation, but Zhou (1995) later modeled IRAS 16293-2422 as collapse with rotation. Zhou et al. (1993) observed B335, a slowly rotating source, and modeled its blue-peaked profiles as inside-out collapse (Shu 1977). André et al. (1993) extended the tripartite taxonomy of young stellar objects to include Class 0 objects (very embedded sources, such as B335 and IRAS 16293). André and Montmerle (1994) found that the Class 0 sources were more embedded than Class I sources and inferred that they had not yet accreted most of their mass. Spectral line surveys of Class 0 sources (Gregersen et al. 1997, Mardones et al. 1997), found nearly a third to half of Class 0 objects displayed asymmetries in optically thick lines like those seen in B335 and IRAS 16293-2422.

However, the earliest phase of the collapse process, the transition between the quasi-static core formation and the beginning of infall onto a central object, is poorly understood. Beichman et al. (1986)

---

<sup>1</sup>Electronic mail: gregerse@physun.physics.mcmaster.ca

<sup>2</sup>Electronic mail: nje@astro.as.utexas.edu

examined the IRAS data for 95 cloud cores previously surveyed by Myers et al. (1983), Myers and Benson (1983) and Benson (1983) in  $^{13}\text{CO}$ ,  $\text{C}^{18}\text{O}$  and  $\text{NH}_3$  and found that half had IRAS sources, which they deduced as arising from protostars. Ward-Thompson et al. (1994) observed 17 cores from Beichman et al. that have no IRAS sources. They detected 12 of these cores in the submillimeter and used maps to study the density profiles of 5 cores. Since these objects lacked IRAS sources, it is believed that protostars have not yet formed. From statistical arguments about the lifetime of these cores and the fact that the observed density profiles are similar to those predicted by ambipolar diffusion models, Ward-Thompson et al. identified these starless cores as in the ambipolar diffusion phase and pre-protostellar. This stage precedes the Class 0 phase and is sometimes referred to as the pre-protostellar core stage.

We observed the objects surveyed by Ward-Thompson et al. using the  $\text{HCO}^+$   $J = 3 - 2$  line, a line that readily displays an asymmetry indicative of protostellar collapse to see if an early collapse phase could be found. Lee et al. (1999) have completed a similar survey using CS and  $\text{N}_2\text{H}^+$  lines.

## 2. OBSERVATIONS AND RESULTS

We observed the 17 starless cores listed in Table 1 in the  $\text{HCO}^+$   $J = 3 - 2$  line with the 10.4-m telescope of the Caltech Submillimeter Observatory (CSO)<sup>3</sup> at Mauna Kea, Hawaii in March 1995, December 1995, June 1996, July 1998, December 1998 and July 1999. We used an SIS receiver (Kooi et al. 1992) with an acousto-optic spectrometer with 1024 channels and a bandwidth of 49.5 MHz as the backend. The frequency resolution ranged from slightly less than 3 channels,  $0.15 \text{ km s}^{-1}$  at 267 GHz, for the 1995 observations to closer to 2 channels,  $0.12 \text{ km s}^{-1}$  at 267 GHz, for the 1998 observations. The antenna temperature,  $T_A^*$ , was obtained from chopper-wheel calibration. Information about the observed lines is listed in Table 2. Planets were used as calibration sources for calculating the main beam efficiency. Data from separate runs were resampled to the resolution of the run with the worst frequency resolution before averaging. A linear baseline was removed before scans were averaged.

Line properties are listed in Table 3. For lines without two clearly distinguished peaks,  $T_A^*$ , the peak temperature,  $V_{LSR}$ , the line centroid, and  $\Delta V$ , the line width, were found by fitting a single Gaussian to the line profile. For lines with two clearly distinguished peaks, we list two values of  $T_A^*$  and  $V_{LSR}$ , one for each peak, and we give one value for the line width, which is the full width across the spectrum at the temperature where the weaker peak falls to half power.

We observed 17 sources in this survey. All of the sources were observed in the  $\text{HCO}^+$   $J = 3 - 2$  line. Six sources were also observed in the  $\text{H}^{13}\text{CO}^+$   $J = 3 - 2$  line. Six sources showed a blue asymmetry in the  $\text{HCO}^+$   $J = 3 - 2$  line (Figure 1). Eight sources showed symmetric lines (Figure 2) and three sources were not detected. The spectra in Figures 1 and 2 are from the central position except that of L1689B which is from  $(-15'', 15'')$ , which we chose because it was the strongest position.

## 3. Individual Sources

---

<sup>3</sup>The CSO is operated by the California Institute of Technology under funding from the National Science Foundation, contract AST 90-15755.

### 3.1. L1498

Wang (1994) observed absorption in the  $\text{H}_2\text{CO}$  6 cm line against the cosmic microwave background radiation similar to that observed in B335. Kuiper et al. (1996) posited that this core is quasi-static or slowly contracting and that the outer envelope is growing. They also concluded that this core could collapse within the next  $5 \times 10^6$  years. Wolkovitch et al. (1997) determined that this core was extremely quiescent based on its narrow CCS line widths. The  $\text{HCO}^+$   $J = 3 - 2$  line (Figure 2) shows no asymmetry and is at the same velocity as the  $\text{N}_2\text{H}^+$  and  $\text{C}_3\text{H}_2$  lines observed by Benson et al. (1998).

### 3.2. L1506

The  $\text{HCO}^+$   $J = 3 - 2$  spectrum (Figure 2) shows one component at  $7.5 \text{ km s}^{-1}$  with a possible second component at  $9 \text{ km s}^{-1}$ .

### 3.3. L1517C

The  $\text{HCO}^+$   $J = 3 - 2$  line (Figure 2) is too weak to detect an asymmetry.

### 3.4. L1517A

We observe a slight blue shoulder in  $\text{HCO}^+$   $J = 3 - 2$  (Figure 2).

### 3.5. L1512

Caselli et al. (1995) observed the hyperfine components of the  $\text{N}_2\text{H}^+$   $J = 1 - 0$  line and found that a single excitation temperature could not fit the spectra, an anomaly usually seen in starless cores. The  $\text{HCO}^+$   $J = 3 - 2$  line (Figure 2) is symmetric and is at the same velocity as the  $\text{N}_2\text{H}^+$  and  $\text{C}_3\text{H}_2$  lines (Benson et al. 1998).

### 3.6. L1544

Myers et al. (1996) modeled the  $\text{H}_2\text{CO}$   $J = 2_{12} - 1_{11}$  line as arising from infall. Tafalla et al. (1998) found that their CS  $J = 2 - 1$  observations could be modeled as arising from inward motions, but those inward motions are not consistent with the predictions of the Shu (1977) inside-out collapse model. Williams

et al. (1999) observed similar infall speeds in  $\text{N}_2\text{H}^+ J = 1 - 0$  on scales of  $10''$  to those observed by Tafalla et al. Ohashi et al. (1999) mapped this core in  $\text{CCS } J_N = 3_2 - 2_1$  and observed both infall and rotational motion. Ciolek and Basu (2000) have modeled the observations of Tafalla et al. and Williams et al. in the context of ambipolar diffusion. The  $\text{HCO}^+ J = 3 - 2$  spectrum is blue-peaked with the  $\text{H}^{13}\text{CO}^+ J = 3 - 2$  line peaking in the dip (Figure 1). The  $\text{N}_2\text{H}^+$  peaks between the  $\text{H}^{13}\text{CO}^+$  line and the  $\text{HCO}^+$  peak while the  $\text{C}_3\text{H}_2$  peaks on the  $\text{H}^{13}\text{CO}^+$  line (Benson et al.).

### 3.7. L1582A

The  $\text{HCO}^+ J = 3 - 2$  line is symmetric (Figure 2). The  $\text{N}_2\text{H}^+$  line of Benson et al. has the same peak velocity as the  $\text{HCO}^+$  line. There is a hint of a blue shift relative to the  $\text{N}_2\text{H}^+$  velocity, but not enough to warrant inclusion as an infall candidate.

### 3.8. L134A

The  $\text{HCO}^+ J = 3 - 2$  spectra displays a symmetric line (Figure 2). The  $\text{N}_2\text{H}^+$  and  $\text{C}_3\text{H}_2$  lines (Benson et al.) peak at the blue edge of our  $\text{HCO}^+$  line. Because those lines were observed  $115''$  from our position, we disregard this source in the statistical discussion in §4.2.

### 3.9. L183

Fulkerson and Clark (1984) used the  $\text{H}_2\text{CO}$  6 cm line to model the density distribution as an inverse square law. The  $\text{CS } J = 2 - 1$  line observed by Snell et al. (1982) is similar in velocity and shape to our  $\text{HCO}^+ J = 3 - 2$  spectra (Figure 1). The  $\text{HCO}^+ J = 3 - 2$  line is self-absorbed with the blue peak slightly stronger. The  $\text{H}^{13}\text{CO}^+$ ,  $\text{N}_2\text{H}^+$  and  $\text{C}_3\text{H}_2$  lines (Benson et al.) peak in the self-absorption dip.

### 3.10. L1696A

The  $\text{HCO}^+ J = 3 - 2$  line is symmetric with a faint blue shoulder (Figure 2). The peak velocity corresponds to that of the optically thin lines of Benson et al.

### 3.11. L1689A

We observe a broad, blue-skewed line in  $\text{HCO}^+ J = 3 - 2$  (Figure 1).

### 3.12. L1689B

The spectra for the  $\text{HCO}^+ J = 3 - 2$  line is blue skewed with the  $\text{H}^{13}\text{CO}^+ J = 3 - 2$  line peaking to the red of the peak velocity of the  $\text{HCO}^+$  line (Figure 1).

### 3.13. L63

The  $\text{HCO}^+ J = 3 - 2$  line is strongly blue-skewed and the  $\text{H}^{13}\text{CO}^+$  line peaks in the middle of the  $\text{HCO}^+$  line (Figure 1). The  $\text{N}_2\text{H}^+$  and  $\text{C}_3\text{H}_2$  lines (Benson et al.) are at the velocity of the red edge of the blue peak.

### 3.14. B133

Hong et al. (1991) have mapped this core in  $^{12}\text{CO}$  and  $^{13}\text{CO } J = 1 - 0$ . The  $\text{HCO}^+ J = 3 - 2$  line is slightly blue-skewed (Figure 1). The  $\text{N}_2\text{H}^+$  and  $\text{C}_3\text{H}_2$  lines of Benson et al. peak at the red edge of the blue peak.

### 3.15. Nondetections

The  $\text{HCO}^+ J = 3 - 2$  line was not detected down to a limit of 0.05 K in L1495D, L1521A and L1517D.

## 4. ANALYSIS

### 4.1. New collapse candidates in $\text{HCO}^+$

Six of these cores, L1544, L1689A, L1689B, L183, L63 and B133, have line profiles with blue asymmetry. A blue asymmetry in an optically thick line like  $\text{HCO}^+ J = 3 - 2$  can be caused by protostellar collapse (Leung and Brown 1977, Zhou & Evans 1994). We observed  $\text{H}^{13}\text{CO}^+ J = 3 - 2$  in all of these sources to find the rest velocity and we also used the  $\text{N}_2\text{H}^+$  and  $\text{C}_3\text{H}_2$  observations of Benson et al. to provide optically thin line velocities. If optically thin lines have the same velocity as the dip of the double-peaked line, the dip is self-absorption from the ambient cloud and not caused by two separate velocity components blended together.

For such narrow lines as seen in these sources, the rest frequencies of lines become an issue. The frequency of the  $\text{HCO}^+ J = 3 - 2$  line is known to within an uncertainty of 0.01 MHz, but the uncertainty of the  $\text{H}^{13}\text{CO}^+ J = 3 - 2$  is potentially large. The standard value in the JPL data base (Pickett et al. 1998,

<http://spec.jpl.nasa.gov>) is 260.255478 GHz. It is calculated from measurements of the two lower lines (Woods et al. 1976, Bogey et al. 1981), making it impossible to estimate uncertainties in the  $J = 3 - 2$  line frequency. Comparing the velocities of sources done in  $\text{H}^{13}\text{CO}^+$  here and elsewhere (Gegersen et al. 1997, 2000) with line velocities of the same sources in  $\text{N}_2\text{H}^+$ , on average the  $\text{H}^{13}\text{CO}^+$  line is  $0.16 \pm 0.04 \text{ km s}^{-1}$  to the red of the  $\text{N}_2\text{H}^+$  line. Since it is unlikely that the  $\text{H}^{13}\text{CO}^+$  would be consistently red-shifted from the  $\text{N}_2\text{H}^+$ , we have shifted our  $\text{H}^{13}\text{CO}^+$  spectra by  $0.16 \text{ km s}^{-1}$  to the blue and propose a frequency of  $260.255617 \pm 0.000035 \text{ GHz}$  for the  $\text{H}^{13}\text{CO}^+$   $J = 3 - 2$  line, 0.139 MHz higher than the standard value.

For four of these sources, L1544, B133, L183 and L1689B, the  $\text{H}^{13}\text{CO}^+$  line does peak in the self-absorption dip, one of the conditions that must be met before a core can be called a candidate for protostellar collapse. In L63, the  $\text{H}^{13}\text{CO}^+$  coincides with the dip but the  $\text{N}_2\text{H}^+$  lies between the dip and the red peak. We did not detect  $\text{H}^{13}\text{CO}^+$  in L1689A, so we cannot make a claim about its quality as a collapse candidate.

How do the conclusions from  $\text{HCO}^+$  compare to those of Lee et al. (1999) who observed CS and  $\text{N}_2\text{H}^+$ ? They did not observe B133 or L1689A, but they found L1544, L1689B and L183 (their position for L183B is closest to the core we call L183) to be infall candidates. There are slight differences between the CS and  $\text{HCO}^+$  spectra. L1689B has a blue peak with a red shoulder in  $\text{HCO}^+$  and double-peaked profile with a strong blue peak in CS. L1544 has a strong blue peak in  $\text{HCO}^+$  but two peaks of equal strength in CS. L183 has similarly shaped spectra in both lines. Lee et al. (1999) observed a red peaked profile in L63, but their position differs substantially from ours. In general, the different tracers agree reasonably well.

## 4.2. Line profile statistics

Optically thick lines in collapsing sources show a double-peaked line profile with the blue peak stronger than the red peak. There are two ways of quantifying the asymmetry of the line. One could use the ratio of the strengths of the two peaks or the asymmetry parameter (Mardones et al. 1997),  $\delta V = (V_{thick} - V_{thin}) \Delta v_{thin}$ , where  $V_{thick}$  is the velocity of the peak of the optically thick line,  $V_{thin}$  is that of the optically thin line and  $\Delta v_{thin}$  is the linewidth of the optically thin line. We list the results in Table 4. We do not list the results for all the objects where  $\text{HCO}^+$  was observed but only those objects for which we were able to establish a rest velocity from  $\text{H}^{13}\text{CO}^+$ ,  $\text{N}_2\text{H}^+$  or  $\text{C}_3\text{H}_2$ . L134A is listed in parentheses because its  $\text{N}_2\text{H}^+$  spectrum was observed  $115''$  from our  $\text{HCO}^+$  spectrum. All the other sources for which we used the  $\text{N}_2\text{H}^+$  line to determine the asymmetry were observed within  $40''$  of our  $\text{HCO}^+$  position. In Table 5, we list the number of blue, symmetric, and red sources as determined by the asymmetry parameter and visual inspection of the line profiles. Following the classification of Mardones et al. sources with asymmetry  $< -0.25$  are blue, while those with asymmetry  $> 0.25$  are red. The excess, which characterizes how blue is a sample of objects, is the number of blue sources minus the number of red sources divided by the total number of sources. The excess as determined from the asymmetry parameter leaving aside L134A is 0.66, higher than those derived for samples of Class 0 and I sources, 0.25 and 0.39 respectively, using the  $\text{HCO}^+$   $J = 3 - 2$  line (Gegersen et al. 2000). Because the number of sources in our sample is small, it is unclear whether the larger excess is significant, but it appears to be at least as large as in the later stages. Lee et al. found the mean  $\delta V$  of starless cores to be  $-0.24 \pm 0.04$  not so different from the mean  $\delta V$  for Class 0 sources,  $-0.28 \pm 0.10$  (Mardones et al.). For the  $\text{HCO}^+$  observations of all three categories, the mean  $\delta V$  using the  $\text{H}^{13}\text{CO}^+$   $J = 3 - 2$  line frequency proposed in the previous section are  $-0.34 \pm 0.13$ ,  $-0.11 \pm 0.09$  and  $-0.17 \pm 0.08$  for starless cores, Class 0 and Class I objects, respectively. So on the basis of

line asymmetries, these starless cores cannot be distinguished from an older, protostellar population.

### 4.3. Are these young sources?

Zhou (1992) modeled CS lines in cores that have not yet formed a protostar but are evolving toward the singular isothermal sphere, the starting point of the Shu (1977) collapse model. He found CS lines with no asymmetry, narrow line widths that increased after collapse began and peak line temperatures that increase until collapse begins. Gregersen et al. (1997) did evolutionary models of  $\text{HCO}^+ J = 3 - 2$  in collapsing clouds and found that such line parameters as peak temperature, line width, and blue-red asymmetry increase with time to a maximum value and then decline. Therefore, if we observed sources that were just beginning to collapse, these sources would have  $\text{HCO}^+ J = 3 - 2$  lines that have slight asymmetry, small peak temperatures and narrow line widths. If we extend these results backward to  $t = 0$ , to the beginning of collapse, we should expect similar line parameters to those of Zhou (1992). Also, since the luminosity of the protostar does not rise immediately, there is some time after collapse begins but before a source would have been detected by IRAS, so the early stages of the evolutionary models of Gregersen et al. could be applied to “pre-protostellar” objects. In these models, important processes like cloud chemistry and protostellar heating that increase the line width and peak temperatures are glossed over or simplified, so the resulting evolutionary “tracks” are best seen as rough sketches of line parameter evolution. In Figure 3, we plot peak temperature and linewidth versus the blue-red ratio for the two abundance distributions modeled in Gregersen et al. The evolutionary “tracks” in both plots go roughly from the lower left corner to the upper right. We see that the starless cores are congregated toward the lower (i.e. “younger”) half of the plot and the Class 0 and I sources which have IRAS sources extend further to the upper ends of the two plots.

However, there are indications that some of these sources have already begun to collapse in a different way than the Shu model predicts. Several of the starless cores have blue/red ratios that are too large for early collapse and more like the extreme blue-red ratios seen in more evolved Class 0 sources. In fact, B133 displays the most extreme ratio between the blue and red peak of any source in any class. The blue-red ratios for this and other sources are too high to arise in a Shu model. Mardones (1998) modeled several alternative velocity fields and found that a model in which the entire cloud collapses produces the highest blue-red ratio. These large blue-red ratios are further discussed in the next section.

### 4.4. Extended infall signatures

We have partially mapped five cores that showed asymmetric line profiles to observe the extent of the asymmetry. The blue-skewed profiles typically stretch over a large area for such young cores. For example, in L1689B (Figure 4), the self-absorption or blue-skewed lines stretches over roughly 0.04 by 0.03 parsecs. There are some red profiles in the southeast area of the map. For L63 (Figure 5), the blue skewness is seen in an area 0.07 by 0.03 parsecs. We show these two cores because these are the largest maps we have done with good signal-to-noise. Tafalla et al. (1998) have commented on this large extent of the infall signature in L1544 (map in Figure 6). They showed that if L1544 was undergoing inside-out collapse, it would have

produced a protostar easily visible to IRAS and that such an early, large-scale infall does not fit with most theories of protostellar collapse.

These observations of extended infall signatures in  $\text{HCO}^+$  combined with the extreme blue-red ratios mentioned in the last section strengthen the case for extended inward motions. Myers and Lazarian (1998) have proposed that turbulent dissipation in a cloud produces an overall implosion starting from the core exterior as an explanation for extended infall signatures. Alternatively, Li (1999) has found evidence for extended inward motions at speeds up to half the sound speed in calculations of core formation in weakly magnetized clouds. Similar speeds also appear in the model of Ciolek and Basu (2000).

#### 4.5. Starless or Pre-protostellar?

The question of whether to call these cores starless or pre-protostellar is a thorny one. While these cores have no IRAS sources and so can all be called starless, the term pre-protostellar implies that the future evolution of these objects can be definitely predicted. However, we can use the submillimeter observations of Ward-Thompson et al. (1994) to divide the sample into those cores detected by Ward-Thompson et al. at one or more wavelengths and those not detected at all (Table 6). Of the 12 cores in the first group, 6 display blue asymmetry while the other six have no asymmetry. The six cores that display blue asymmetry are the strongest in the submillimeter continuum. Of the 5 cores Ward-Thompson et al. did not detect, 2 have symmetric profiles while we did not detect the other 3 in  $\text{HCO}^+$ . The 2 detections of these cores were among the weakest lines observed. We also include the  $\text{NH}_3$  observations of Benson and Myers (1989) as a marker of dense core evolution. Of the 12 cores with submillimeter emission, all were observed in  $\text{NH}_3$ . Of the 5 others, only one was observed. Five of the cores in the first group have since been mapped in the submillimeter continuum (Shirley et al. 2000). The four most centrally condensed cores show blue asymmetry. The least centrally condensed core, L1512, has no asymmetry in  $\text{HCO}^+$ .

There is a clear distinction between those cores with submillimeter continuum and those without. The first group has stronger line emission that often shows what could be the beginning of infall. The group with relatively strong submillimeter continuum,  $\text{HCO}^+$ , and  $\text{NH}_3$  emission are the likeliest to be pre-protostellar in nature, consistent with the suggestion by Ward-Thompson et al. (1994).

The cores with weak submillimeter continuum could eventually form stars but were undetected simply because of lower column density. These cores may be in an even earlier evolution stage in which cores are just beginning to form, or these cores may be forming stars of lower mass. If these cores are weakly centrally concentrated, they would not have a sufficient excitation temperature gradient for infall asymmetry. Further observations would be needed to resolve the nature of these objects.

## 5. CONCLUSIONS

We have observed 17 starless cores in  $\text{HCO}^+ J = 3 - 2$  in search of the spectral signature of pre-protostellar collapse. These objects do seem to be a younger population than the Class 0 sources based on their narrow line widths and weak peak temperatures. We have observed blue asymmetric line profiles in 6 of these cores, and we suggest L1544, L1689B, B133 and L183 as good protostellar collapse candidates and



L1689A and L63 as worthy of further observations in the  $\text{H}^{13}\text{CO}^+$   $J = 3 - 2$  line. The blue excess of this sample is as prominent as in samples of “older” Class 0 and I sources, suggesting that infalling protostars are not exclusively to be found among the Class 0 sources. A population of likely pre-protostellar cores can be distinguished by their strong submillimeter continuum and  $\text{HCO}^+$  and  $\text{NH}_3$  spectral line emission.

However, recently Tafalla et al. (1998) have found that L1544 cannot be described as inside-out collapse. If infall is happening in that core, it cannot be explained by any current infall model, suggesting that further study of these cores can tell us about the very beginning of the collapse process.

We would like to thank Tommy Greathouse, Wenbin Li, Byron Mattingly and Yancy Shirley for their help with observations. We thank the referee for helpful suggestions, one of which led us to reconsider the rest frequency for the  $\text{H}^{13}\text{CO}^+$  line. This work was supported by NSF grant AST-9317567 and NASA grant NAG5-7203.

## REFERENCES

- André, P. & Montmerle, T. 1994, *ApJ*, 420, 837
- André, P., Ward-Thompson, D., & Barsony, M. 1993, *ApJ*, 406, 122
- Beichman, C. A., Myers, P. C., Emerson, J. P., Harris, S., Mathieu, R., Benson, P. J., & Jennings, R. E. 1986, *ApJ*, 307, 337
- Benson, P. J. 1983, PhD thesis, MIT
- Benson, P. J., Caselli, P., & Myers, P. C. 1998, *ApJ*, 506, 743
- Bogey, M., Demuyck, C., & Destombes, J. L. 1981, *Mol. Phys.* 43, 1043
- Caselli, P., Myers, P. C., & Thaddeus, P. 1995, *ApJ*, 455, L77
- Ciolek, G. E. & Basu, S. 2000, *ApJ*, in press (astro-ph/9909429)
- Fulkerson, S. A. & Clark, F. O. 1984, *ApJ*, 287, 723
- Gregersen, E. M., Evans, N. J., II, Zhou, S., & Choi, M. 1997, *ApJ*, 484, 256
- Gregersen, E. M., Evans, N. J., II, Mardones, D., & Myers, P. C. 2000, *ApJ*, in press (astro-ph/9912175)
- Hong, S. S., Kim, H. G., Park, S. H., Park, Y. S., & Imaoka, K. 1991, *JKAS*, 24, 71
- Kooi, J. W., Chan, M., Phillips, T. G., Bumble, B., & LeDuc, H. G. 1992, *IEEE Transactions on Microwave Theory and Techniques*, 40, 812
- Kuiper, T. B. H., Langer, W. D., & Velusamy, T. 1996, *ApJ*, 468, 761
- Lee, C. W., Myers, P. C., Tafalla, M. 1999, *ApJ*, 526, 788
- Leung, C. M. & Brown, R. L. 1977, *ApJ*, 214, L73
- Li, Z. Y. 1999, *ApJ*, in press (astro-ph/9907358)
- Mardones, D. 1998, PhD thesis, Harvard University
- Mardones, D., Myers, P. C., Tafalla, M., Wilner, D. J., Bachiller, R., & Garay, G. 1997, 489, 719
- Menten, K. M., Serabyn, E., Gusten, R., & Wilson, T. L. 1987, *A&A*, 177, L57
- Myers, P. C. & Benson, P. J. 1983, *ApJ*, 266, 309
- Myers, P. C. & Lazarian, A. 1998, *ApJ*, 507, L157
- Myers, P. C., Linke, C., & Benson, P. J. 1983, *ApJ*, 264, 517
- Myers, P. C., Mardones, D., Tafalla, M., Williams, J. P., & Wilner, D. J. 1996, *ApJ*, 465, L133
- Ohashi, N., Lee, S. W., Wilner, D. J., & Hayashi, M. 1999, *ApJ*, 518, L41
- Pickett, H. M., Poynter, R. L., Cohen, E. A., Delitsky, M. L., Pearson, J. C., & Muller, H. S. P. 1998, *J. Quant. Spectrosc. & Rad. Transfer*, 60, 883
- Shirley, Y. L., Evans, N. J., II, Rawlings, J. M. C., & Gregersen, E. M., 2000, submitted to *ApJ*
- Shu, F. H. 1977, *ApJ*, 214, 488
- Snell, R., Langer, W. D., & Frerking, M. A. 1982, *ApJ*, 255, 149
- Tafalla, M., Mardones, D., Myers, P. C., Caselli, P., Bachiller, R., & Benson, P. J. 1998, *ApJ*, 504, 900
- Walker, C. K., Lada, C. J., Young, E. T., Maloney, P. R., & Wilking, B. A. 1986, *ApJ*, 309, L47

- Wang, Y. 1994. PhD thesis, University of Texas at Austin
- Ward-Thompson, D., Scott, P. F., Hills, R. E., & André, P. 1994, MNRAS, 268, 276
- Williams, J. P., Myers, P. C., Wilner, D. J., & Di Francesco, J. 1999, ApJ, 513, L61
- Wolkovitch, D., Langer, W. D., Goldsmith, P. F., & Heyer, M. 1997, ApJ, 477, 241
- Woods, R. C., Saykally, R. J., Dixon, T. A., Szanto, P. G., & Anderson, T. 1976, 31st Symposium on Molecular Spectroscopy, Columbus, Ohio
- Zhou, S. 1992, ApJ, 394, 204
- Zhou, S. 1995, ApJ, 442, 685
- Zhou, S. & Evans, N. J., II 1994, in Clouds, Cores, and Low Mass Stars, ed. D. P. Clemens & R. Barvainis, San Francisco: Astron. Soc. Pacific, 183
- Zhou, S., Evans, N. J., II, Kompe, C., & Walmsley, C. M. 1993, ApJ, 404, 232

Table 1. List of Sources

Name	R.A. (1950.0)	Dec. (1950.0)	Offpos <sup>a</sup> (")	Distance (pc)	450 $\mu$ m <sup>b</sup> (mJy)	800 $\mu$ m (mJy)	1.1 mm (mJy)	1.3 mm (mJy)
L1498	04:07:50.0	25:02:31	(-1200,0)	140	700 $\pm$ 80	120 $\pm$ 18	35 $\pm$ 6	10 $\pm$ 2.5
L1495D	04:11:15.5	28:07:20	(-900,0)	140	-	<135	<44	<30
L1506	04:15:30.3	25:13:22	(-900,0)	140	-	<66	<48	-
L1521A	04:23:38.4	26:09:27	(-900,0)	140	-	<110	<80	-
L1517C	04:51:35.9	30:30:00	(-900,0)	140	836 $\pm$ 160	100 $\pm$ 20	<83	<7.5
L1517A	04:51:54.8	30:28:53	(-900,0)	140	1280 $\pm$ 330	105 $\pm$ 18	<60	<5.4
L1517D	04:52:36.5	30:34:02	(-900,0)	140	<4500	<120	<130	-
L1512	05:00:54.4	32:39:37	(-900,0)	140	<6000	107 $\pm$ 21	45 $\pm$ 9	<16
L1544	05:01:13.1	25:06:36	(-900,0)	140	1300 $\pm$ 240	450 $\pm$ 58	193 $\pm$ 30	46 $\pm$ 4
L1582A	05:29:14.6	12:28:08	(-900,0)	140	<1240	160 $\pm$ 27	<54	<30
L134A	15:51:05.6	-04:26:10	(-900,0)	150	-	<60	-	<163
L183	15:51:32.7	-02:42:19	(600,0)	150	<1500	269 $\pm$ 30	108 $\pm$ 26	<134
L1696A	16:25:30.0	-24:13:22	(0,-1200)	125	800 $\pm$ 160	105 $\pm$ 18	62 $\pm$ 12	<58
L1689A	16:29:10.5	-24:57:22	(0,-900)	125	2200 $\pm$ 300	290 $\pm$ 45	<102	54 $\pm$ 15
L1689B	16:31:47.0	-24:31:45	(0,-900)	125	<3000	362 $\pm$ 40	140 $\pm$ 34	134 $\pm$ 11
L63	16:47:19.4	-18:01:16	(0,-900)	125	1600 $\pm$ 200	367 $\pm$ 23	<93	<96
B133	19:03:27.3	-06:57:00	(0,-600)	400	<1800	341 $\pm$ 63	<120	<56

<sup>a</sup>The off position used for position switching.

<sup>b</sup>All photometry from Ward-Thompson et al. (1994).

Table 2. List of Observed Lines

Molecule	Transition	Beamwidth ( $''$ )	$\eta_{mb}$	Resolution ( $\text{km s}^{-1}$ )	Frequency (MHz)
$\text{H}^{13}\text{CO}^+$	$J = 3 - 2$	26	0.66	0.15	260255.617 (0.035)
$\text{HCO}^+$	$J = 3 - 2$	26	0.66	0.16	267557.620 (0.01)

Table 3. Results

Source	Line	$T_A^*$ (K)	$V_{LSR}$ (km s <sup>-1</sup> )	$\Delta V$ (km s <sup>-1</sup> )
L1498	HCO <sup>+</sup> $J = 3 - 2$	0.48±0.04	7.81±0.02	0.51±0.04
L1495D	HCO <sup>+</sup> $J = 3 - 2$	<0.05	–	–
L1506	HCO <sup>+</sup> $J = 3 - 2$	0.20±0.03	7.47±0.02	0.38±0.07
L1521A	HCO <sup>+</sup> $J = 3 - 2$	<0.05	–	–
L1517C	HCO <sup>+</sup> $J = 3 - 2$	0.21±0.05	5.63±0.03	0.28±0.09
L1517A	HCO <sup>+</sup> $J = 3 - 2$	0.26±0.05	5.72±0.04	0.70±0.10
L1517D	HCO <sup>+</sup> $J = 3 - 2$	<0.05	–	–
L1512	HCO <sup>+</sup> $J = 3 - 2$	0.41±0.04	7.05±0.02	0.45±0.04
L1544	H <sup>13</sup> CO <sup>+</sup> $J = 3 - 2$	0.09±0.02	7.18±0.04	0.50±0.10
-	HCO <sup>+</sup> $J = 3 - 2$	1.11±0.07	6.96±0.06	0.60±0.12
-	-	0.91±0.07	7.44±0.06	-
L1582A	HCO <sup>+</sup> $J = 3 - 2$	0.77±0.05	10.06±0.02	0.83±0.04
L134A	HCO <sup>+</sup> $J = 3 - 2$	0.23±0.04	2.93±0.04	0.44±0.11
L183	H <sup>13</sup> CO <sup>+</sup> $J = 3 - 2$	0.08±0.02	2.67±0.04	0.43±0.09
-	HCO <sup>+</sup> $J = 3 - 2$	0.28±0.01	2.27±0.08	0.96±0.16
-	–	0.25±0.01	2.75±0.08	–
L1696A	HCO <sup>+</sup> $J = 3 - 2$	0.91±0.06	3.45±0.01	0.43±0.03
L1689A	H <sup>13</sup> CO <sup>+</sup> $J = 3 - 2$	<0.03	–	–
–	HCO <sup>+</sup> $J = 3 - 2$	0.53±0.03	3.57±0.02	1.13±0.04
L1689B	H <sup>13</sup> CO <sup>+</sup> $J = 3 - 2$	0.23±0.03	3.41±0.02	0.50±0.06
–	HCO <sup>+</sup> $J = 3 - 2$	1.12±0.07	3.33±0.01	0.58±0.04
L63	H <sup>13</sup> CO <sup>+</sup> $J = 3 - 2$	0.12±0.03	5.73±0.06	0.71±0.24
–	HCO <sup>+</sup> $J = 3 - 2$	1.07±0.03	5.53±0.08	0.60±0.15
B133	H <sup>13</sup> CO <sup>+</sup> $J = 3 - 2$	0.12±0.03	12.27±0.04	0.38±0.07
–	HCO <sup>+</sup> $J = 3 - 2$	0.63±0.03	12.01±0.01	0.57±0.03

Table 4. Line Asymmetry

Source	Blue/Red	Asymmetry
L1498	–	-0.04±0.09
L1512	–	-0.32±0.12
L1544	1.22±0.12	-0.44±0.17
L1582A	–	-0.35±0.06
L134A	–	(0.95±0.21)
L183	1.12±0.06	-0.93±0.28
L1696A	–	0.12±0.06
L1689A	1.23±0.11	–
L1689B	2.48±0.38	-0.16±0.05
L63	1.55±0.08	-0.28±0.16
B133	3.14±0.45	-0.68±0.17

<sup>a</sup>The asymmetry for L134A was calculated from N<sub>2</sub>H<sup>+</sup> spectra (Benson et al. 1999) observed 115'' from our HCO<sup>+</sup> position.

Table 5. Asymmetry Statistics

Method	Blue	Symmetric	Red	Excess
Asymmetry	6	3	0	0.67
Profiles	6	8	0	0.43



Table 6. Criteria for Pre-Protostellar Cores

Source	Continuum	HCO <sup>+</sup>	NH <sub>3</sub>	Blue profile
L1498	Y	Y	Y	N
L1517C	Y	Y	Y	N
L1517A	Y	Y	Y	N
L1512	Y	Y	Y	N
L1544	Y	Y	Y	Y
L1582A	Y	Y	Y	N
L183	Y	Y	Y	Y
L1696A	Y	Y	Y	N
L1689A	Y	Y	Y	Y
L1689B	Y	Y	Y	Y
L63	Y	Y	Y	Y
B133	Y	Y	Y	Y
L1495D	N	N	N	N
L1506	N	Y	N	N
L1521A	N	N	N	N
L1517D	N	N	N	N
L134A	N	Y	Y	N

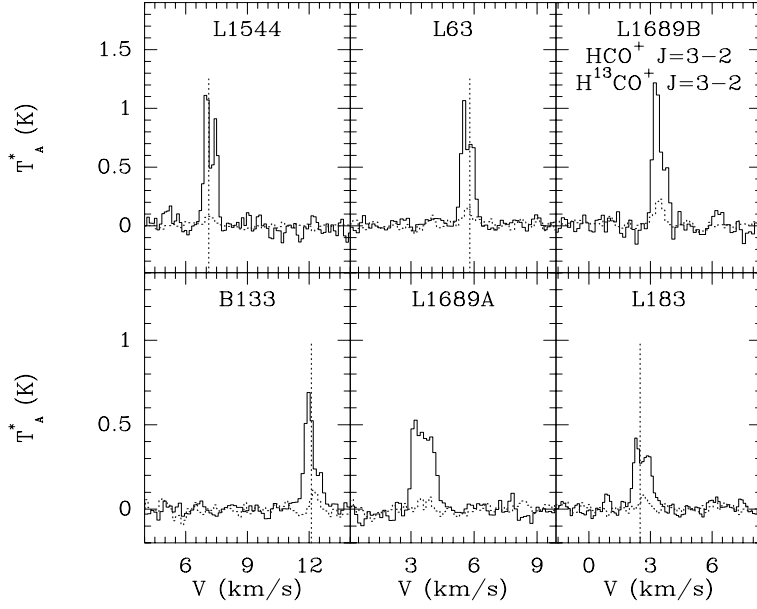


Fig. 1.—  $\text{HCO}^+$  and  $\text{H}^{13}\text{CO}^+$   $J = 3 - 2$  spectra toward the center of six starless cores. The  $\text{HCO}^+$   $J = 3 - 2$  spectra is the solid line and the  $\text{H}^{13}\text{CO}^+$   $J = 3 - 2$  spectra is the dashed line. The dashed vertical line is the velocity of the  $\text{N}_2\text{H}^+$  line of Benson et al. (1998).

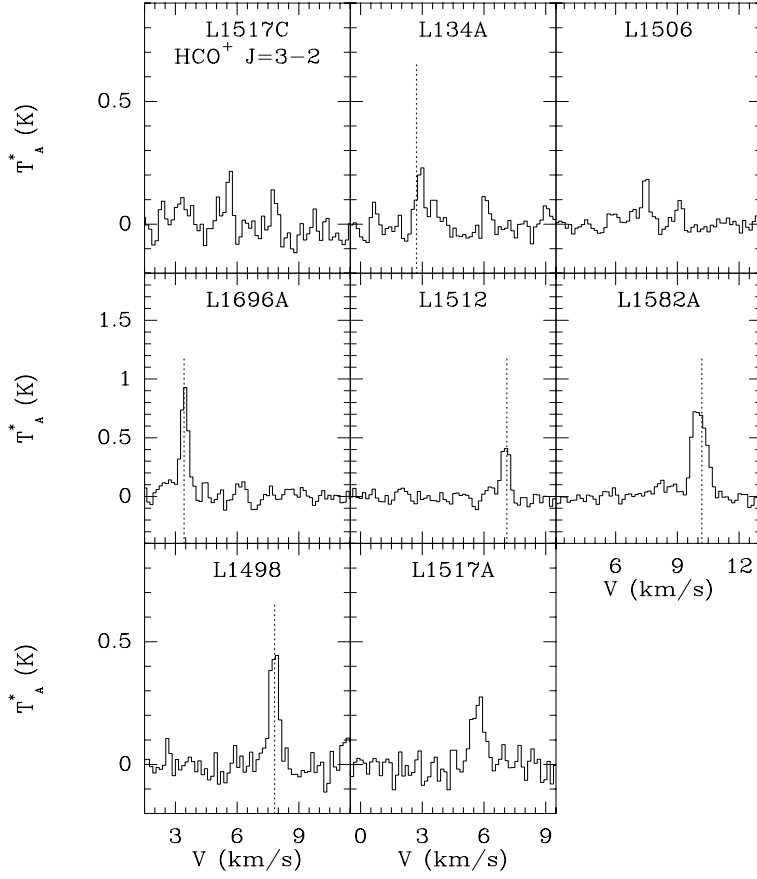


Fig. 2.—  $\text{HCO}^+ J = 3 - 2$  spectra toward the center of eight starless cores. The dashed vertical line is the velocity of the  $\text{N}_2\text{H}^+$  line of Benson et al. (1998).

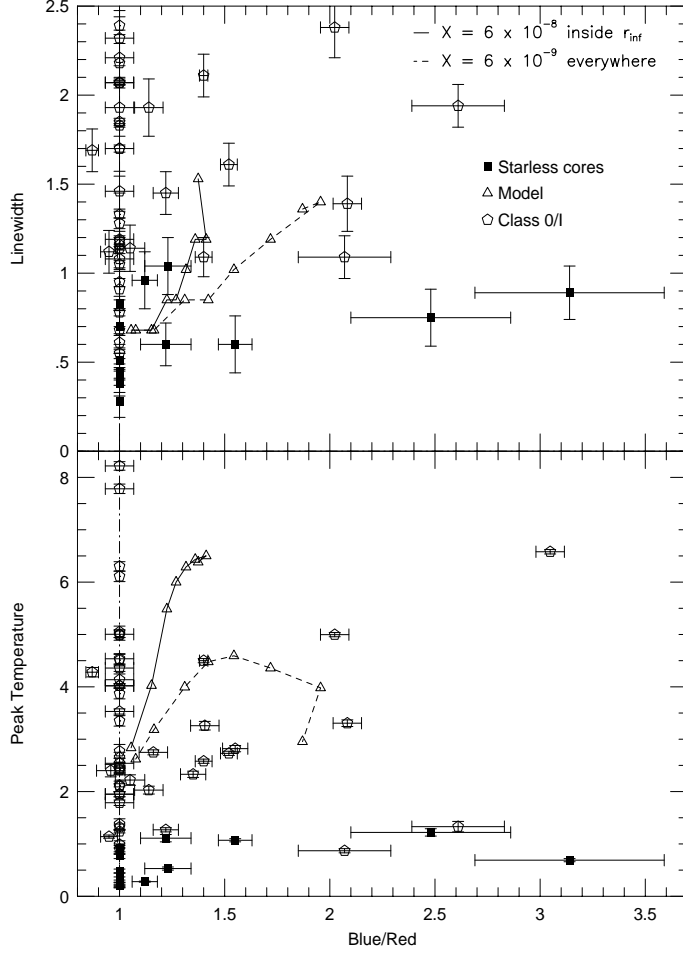


Fig. 3.— The top plot is the peak temperature of the  $\text{HCO}^+ J = 3 - 2$  line versus blue-red asymmetry and the bottom plot is linewidth of the  $\text{HCO}^+ J = 3 - 2$  line versus blue-red asymmetry. Open triangles are points from the evolutionary models of Gregersen et al. (1997). Open triangles connected by a solid line are from infall models with  $X(\text{HCO}^+) = 6 \times 10^{-8}$  inside the infall radius; those connected by a dashed line have  $X(\text{HCO}^+) = 6 \times 10^{-9}$  throughout. Filled squares are the starless cores and the open pentagons are previously observed Class 0 and Class I sources (Gregersen et al. 1997, 2000 respectively).

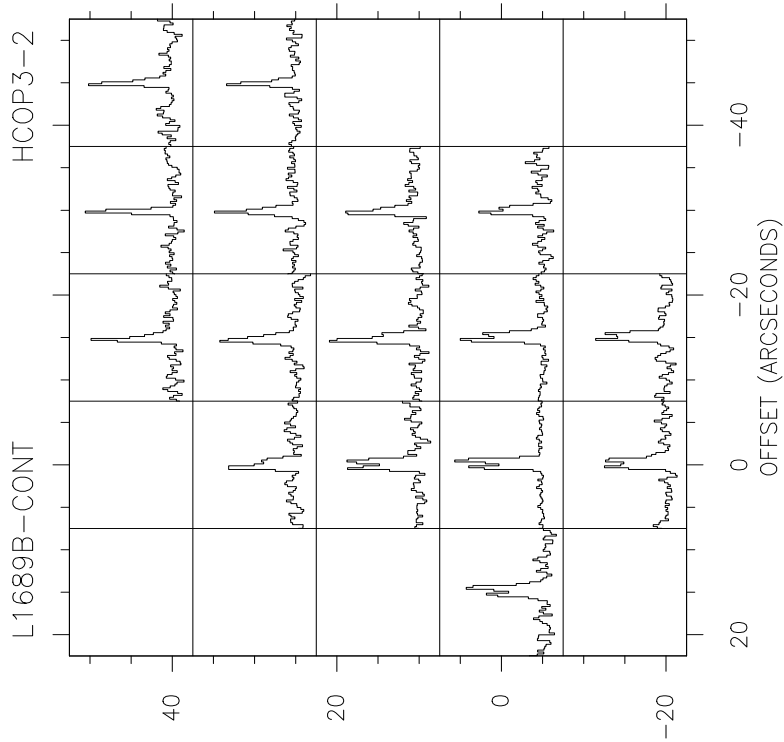


Fig. 4.— Map of  $\text{HCO}^+ J = 3 - 2$  spectra in L1689B. The velocity scale is from  $-1.5$  to  $8.5 \text{ km s}^{-1}$  and the temperature scale is from  $-0.3$  to  $1.4 \text{ K}$ .

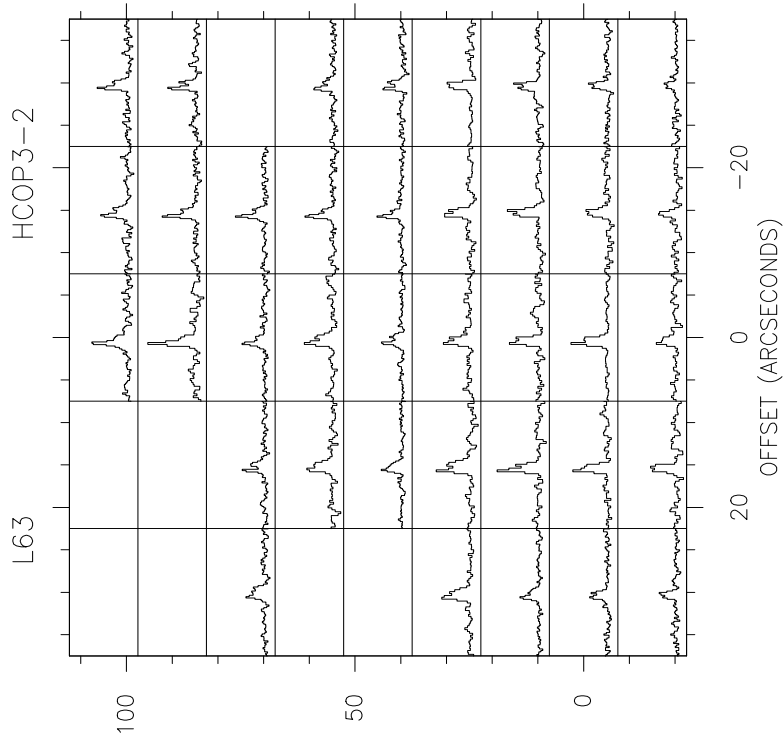


Fig. 5.— Map of  $\text{HCO}^+ J = 3 - 2$  spectra in L63. The velocity scale is from 1 to 11  $\text{km s}^{-1}$  and the temperature scale is from  $-0.3$  to 1.7 K.

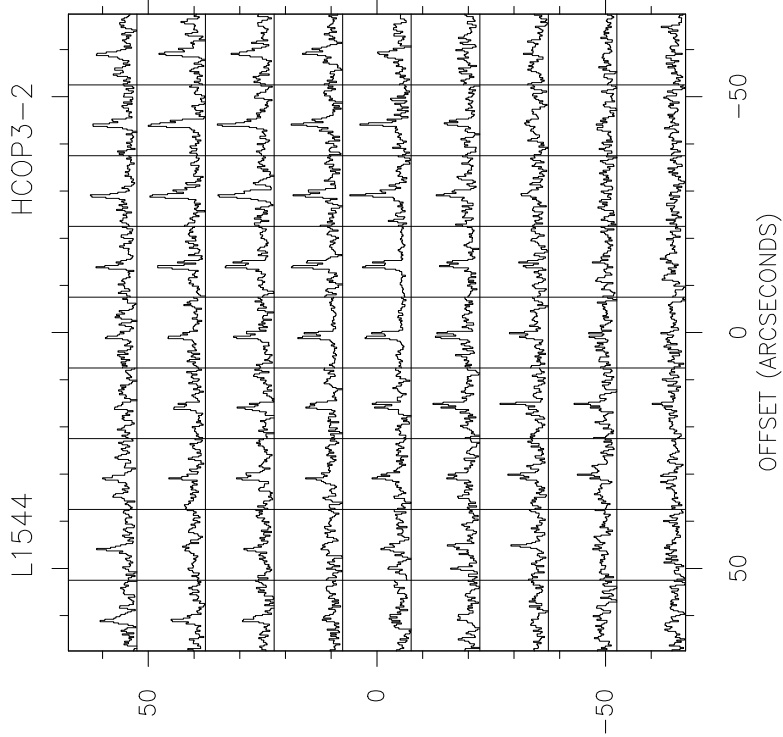


Fig. 6.— Map of  $\text{HCO}^+$   $J = 3 - 2$  spectra in L1544. The velocity scale is from 2.5 to 12.5  $\text{km s}^{-1}$  and the temperature scale is from  $-0.3$  to 1.8 K.